Clays and Clay Minerals, Vol. 62, No. 4, 336–353, 2014.

EXPANSION BEHAVIOR OF OCTADECYLAMMONIUM-EXCHANGED LOW- TO HIGH-CHARGE REFERENCE SMECTITE-GROUP MINERALS AS REVEALED BY HIGH-RESOLUTION TRANSMISSION ELECTRON MICROSCOPY ON ULTRATHIN SECTIONS

DIRK SCHUMANN[1,2,*], REINHARD HESSE[3,4], S. KELLY SEARS[5], AND HOJATOLLAH VALI[3,5]

[1] Fibics Incorporated, 1431 Merivale Road, Suite 100, Lower Level, Ottawa, ON, K2E 0B9, Canada
[2] Department of Earth Sciences, Western University, 1151 Richmond Street N., London, ON, N6A 5B7, Canada
[3] Department of Earth and Planetary Sciences, McGill University, 3450 University Street, Montréal, QC, H3A 0E8, Canada
[4] Department of Geo- and Environmental Sciences, Section Geology, Ludwig Maximilian University, Luisenstr. 37, D-80333, München, Germany
[5] Facility for Electron Microscopy Research, McGill University, 3640 University Street, Montréal, QC, H3A 2B2, Canada

Abstract—Ultrathin sections of reference 2:1 layer silicates treated with octadecylammonium cations were examined using high-resolution transmission electron microscopy (HRTEM) to establish the layer structure. Hitherto, few HRTEM ultrathin-section data existed on the expansion behavior of smectite-group minerals with different interlayer-charge values. Without such information, the expansion behavior of both low-charge and high-charge smectite minerals cannot be characterized and the structures observed in HRTEM images of clay-mineral mixtures cannot be interpreted reliably. Reference smectite-group minerals (Upton, Wyoming low-charge montmorillonite; Otay, California high-charge montmorillonite; a synthetic fluorohectorite; and a Jeanne d'Arc Basin offshore Newfoundland clay sample) with a range of layer charge values were examined. To prevent possible intrusion of epoxy resin into interlayers during embedding, the clay samples were first embedded in epoxy, sectioned with an ultra microtome, and then treated with octadecylammonium cations before examination using HRTEM. Lattice-fringe images showed that lower-charge (<0.38 eq/$O_{10}(OH)_2$) 2:1 layers had 13−14 Å spacings, whereas higher-charge (>0.38 eq/$O_{10}(OH)_2$) 2:1 layers had 21 and 45 Å spacings. These differently expanded silicate layers can occur within the same crystal and an alternation of these layer types can generate rectorite-like structures. For comparison, clay samples were also treated with octadecylammonium before epoxy embedding and sectioning and then examined with HRTEM. These samples mostly had highly expanded interlayers due to epoxy intrusion in the interlayer space. The reference clay minerals embedded in epoxy resin, sectioned, and treated with octadecylammonium cations were used to characterize smectite-group minerals in a natural clay sample from the Jeanne d'Arc Basin, Eastern Canada. Smectite-group minerals in this sample revealed similar structures in lattice-fringe images to those observed in the pure reference clay samples. Rectorite-like structures observed in lattice-fringe images were in fact smectite crystals with short, alternating sequences of low-charge and high-charge smectite layers rather than illite-smectite (I-S) phases with expanded smectite layers and non-expanded 10 Å illite layers.

Key Words—Clay Minerals, High-resolution Transmission Electron Microscopy, Lattice-fringe Images, *n*-alkylammonium Cations, Mixed-layer Illite/smectite, Rectorite-like Structures, Smectite-group Minerals.

INTRODUCTION

Organic compounds such as glycerol and ethylene glycol are commonly used to identify expandable smectite-group clay minerals and to differentiate them from non-expandable clay minerals such as illite and chlorite (MacEwan, 1944; Brindley, 1966). The expansion of the 2:1 layer silicates, caused by the replacement of inorganic interlayer cations by *n*-alkylammonium cations, is used to determine layer-charge magnitude and distribution (Lagaly and Weiss, 1969; 1970a, 1970b, 1970c). This method became a frequently used technique in various subsequent studies to estimate layer charge and charge distribution in expandable 2:1 layer silicates (Lagaly and Weiss, 1971; Stul and Mortier, 1974; Rühlicke and Kohler, 1981, Stanjek and Friedrich, 1986; Laird *et al.*, 1989a; Olis *et al.*, 1990) but limitations and problems associated with the method were also identified (Mermut, 1994). X-ray diffraction (XRD) analysis has been the usual method for routine identification and structural characterization of clay minerals. However, XRD patterns average signals over thousands of unit cells and particles and therefore cannot provide the micro- and nano-scale information required for a reliable identification of clay minerals, particularly of mixed-layer minerals.

Transmission electron microscopy (TEM), however, can be used to obtain this crucial information about clay

* E-mail address of corresponding author:
dschumann@fibics.com
DOI: 10.1346/CCMN.2014.0620407

materials. A detailed review of the preparation methods of clay-mineral and soil samples for TEM investigations was given by Elsass *et al.* (2008). Special preparation techniques have been developed to examine silicate layers perpendicular to the stacking axis direction (Eberhart and Triki, 1972; Lee *et al.*, 1975). The *n*-alkylammonium cation-exchange method was first combined with TEM lattice-fringe imaging of different 2:1 clay-mineral ultrathin sections (Vali and Köster, 1986) to investigate structure and expansion behavior. This approach, in which *n*-alkylammonium cation exchange is performed before clay minerals are embedded in epoxy resin (Figure 1: method 1), was also applied in various other studies (Graf von Reichenbach *et al.*, 1988; Ghabru *et al.*, 1989; Laird *et al.*, 1989b; Laird and Nater, 1993; Malla *et al.*, 1993; Cetin and Huff, 1995).

Previous smectite-group minerals studies (Vali, 1983; Vali and Köster, 1986; Malla *et al.*, 1993) that prepared samples using method 1 always found larger spacings in TEM lattice-fringe images than those determined by XRD analyses (Table 3). The additional expansion observed in TEM images was attributed to incorporation of epoxy resin into clay interlayers during the embedding of *n*-alkylammonium-treated smectite-group minerals in epoxy.

In order to avoid resin infiltration in the interlayer space, Vali and Hesse (1990) developed a new method in which samples are first embedded in epoxy resin. After ultrathin sections are cut and transferred to TEM grids, the treatment with *n*-alkylammonium cations is performed on the ultrathin sections (see Figure 1: method 2, and Table 1). This method was used subsequently in several studies that used HRTEM to examine 2:1 layer silicates from various geological settings. Most clay minerals prepared according to the Vali and Hesse (1990) method (method 2) for HRTEM examination were reference high-charge 2:1 layer silicates (Marblehead Illite, Zempleni Illite, Llano and Jefferson vermiculite) and clay mixtures from various geological environments that contained different proportions of smectite-group minerals, illite, vermiculite, and mica (Vali *et al.*, 1991, 1993, 1994; Vali and Hesse, 1992; Sears *et al.*, 1998; Lee *et al.*, 2003; Shata *et al.*, 2003).

The only reference smectite-group sample prepared for HRTEM examination that was alkylammonium-exchanged after epoxy embedding and sectioning was the SWa-1 nontronite (Vali and Hesse, 1990). No reference smectite-group minerals other than nontronite have been prepared using method 2 and examined with HRTEM (Figure 1). Without knowing the expanding behavior of low-charge and high-charge smectite-group minerals prepared using this method (method 2), however, correct interpretation of the structures in silicate clay-mineral mixtures or explanation of the discrepancies between the *d* values obtained from HRTEM lattice-fringe images and XRD analyses is impossible.

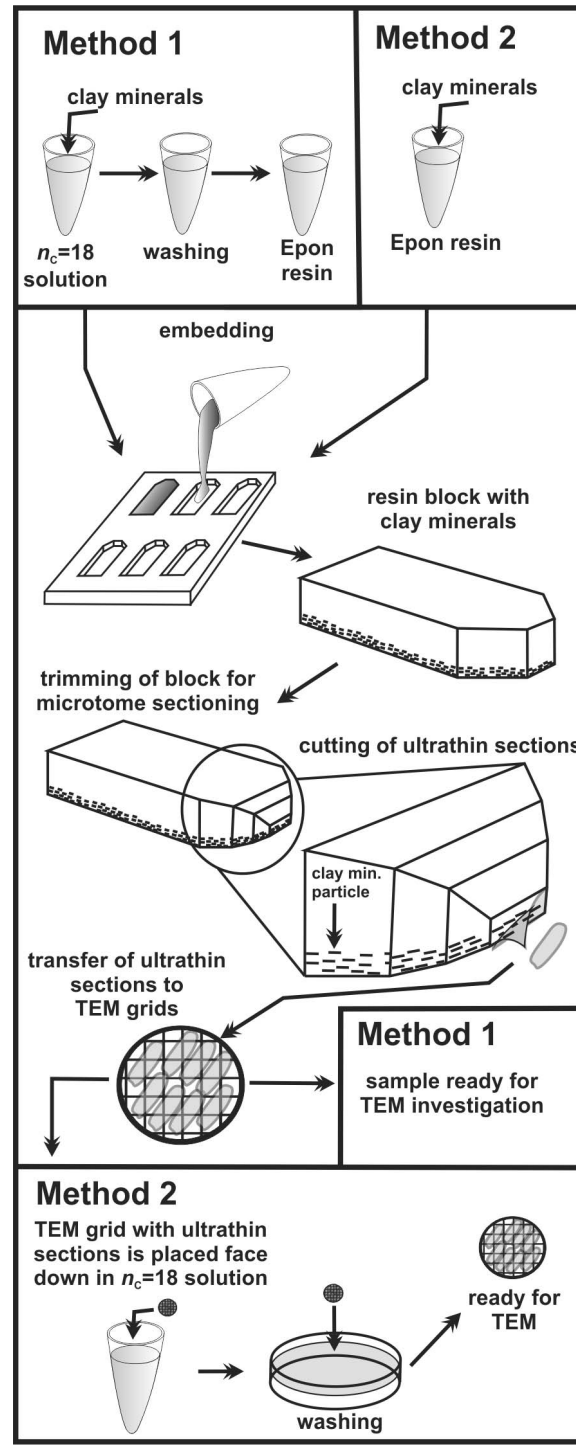

Figure 1. Sample preparation for examination by HRTEM using methods 1 and 2.

The objectives of the present study were, therefore, to: (1) embed in epoxy resin smectite-group minerals with a range of layer charge, prepare stacking axis-parallel ultrathin sections, treat the ultrathin sections

https://doi.org/10.1346/CCMN.2014.0620407 Published online by Cambridge University Press

Table 1. Procedural steps describing the different embedding and octadecylammonium cation-exchange treatment methods on the copper grid as well as the octadecylammonium cation treatment before embedding in epoxy resin.

Sample	Method 1 octadecylammonium cation exchange treatment before embedding			Method 2 octadecylammonium cation exchange treatment after embedding and cutting of ultrathin sections		
	1. exchange	2. washing	3. embedding	1. embedding	2. exchange	3. washing
Upton Montm.	20 minutes					
Upton Montm. Otay Montm. Fluorohectorite (0.4) Fluorohectorite (0.6)	5 days	with 100% ethanol up to 20 times	in Epon resin	in Epon resin	20 min	gently submerge TEM grid in a Petri dish with preheated distilled H_2O (65ºC)

with octadecylammonium (n_C = 18) cations (Figure 1, method 2), examine them with HRTEM; and (2) compare the *d* values obtained from HRTEM lattice-fringe images to *d* values from XRD analyses and HRTEM lattice-fringe *d* values from the same clay samples treated with octadecylammonium before embedding in epoxy resin and sectioning (Figure 1, method 1).

MATERIALS AND METHODS

Samples

The two montmorillonite and two hectorite samples selected as reference materials for this study were Upton montmorillonite from Wyoming (reference No. 25 of the American Petroleum Institute (A.P.I.)), Otay montmorillonite from California (A.P.I. No. 24), and synthetic fluorohectorites. Samples of synthetic fluorohectorite with interlayer charges of 0.4 and 0.6 eq/$O_{10}(OH)_2$ were synthesized and provided by Josef Breu, University of Bayreuth, Germany (Breu *et al.*, 2001; Malikova *et al.*, 2007). The reference clay minerals have the following structural formulae:

Upton montmorillonite:
$R^{n+}_{0.36/n}\ mH_2O\ (Al_{1.58}Fe^{3+}_{0.12}Fe^{2+}_{0.02}Mg_{0.28})$
$[Al_{0.06}Si_{3.94}]O_{10}(OH)_2$ (Vogt and Köster, 1978)

Otay montmorillonite:
$Na_{0.42}Mg_{0.09}Ca_{0.01}mH_2O(Al_{1.35}Fe^{3+}_{0.06}Mg_{0.59})$
$[Al_{0.02}Si_{3.98}]O_{10}(OH)_2$ (Schultz, 1969)

Synthetic fluorohectorite:
$Na_{0.4}mH_2O(Mg_{2.6}Li_{0.4})[Si_{4.0}]O_{10}F_2$ and
$Na_{0.6}mH_2O(Mg_{2.4}Li_{0.6})[Si_{4.0}]O_{10}F_2$.

One argillaceous rock sample from an area that is currently undergoing active burial diagenesis in the Jeanne d'Arc Basin, offshore Newfoundland, Canada, was selected in order to study the <0.1 μm fraction of natural smectite-group minerals. The sample was collected at the core storage facility of the Canada-Newfoundland and Labrador Offshore Petroleum Board (C-NLOPB) in St John's (Newfoundland) from core cuttings that came from the well Adolphus D-50 (AD-D50) (C-NLOPB Schedule of Wells, 2007). The sampled core cuttings were obtained from 2035 m depth from the Paleocene to Pliocene Banquereau Formation that represents the Tertiary passive-margin sediment fill of the Jeanne d'Arc Basin (Sinclair, 1988). The <0.1 μm grain size fraction of this sample was described by Abid *et al.* (2004) as R = 0 randomly interstratified I-S mixed-layer clay minerals with 34% illite in I-S.

The Jeanne d'Arc Basin well cuttings of sample AD-D50 (2035 m) were dispersed and washed several times in distilled water. The <0.1 μm factions of samples AD-D50 (2035 m), Upton montmorillonite, and Otay montmorillonite were separated using a high-speed, bench-top, Beckman Coulter AllegraTM 21R centrifuge at $10730 \times g$ using a fixed-angle rotor. The clay-mineral suspensions were frozen and freeze-dried. The synthetic fluorohectorite material was used as received.

n-alkylammonium cation-exchange method

The *n*-alkylammonium cation-exchange method developed by Lagaly and Weiss (1969) is a tool to determine the interlayer-charge density, layer charge, and charge distribution of expandable 2:1 layer silicates, such as smectites, vermiculite, and illitic minerals in XRD. An *n*-alkylammonium cation consists of an alkyl chain ($C_{n}H_{2n+1}$) and an ammonium group (NH_3^+) with the general formula $C_{n}H_{(2n+1)}NH_3^+$ (n_C = number of carbon atoms in the chain).

Alkylammonium-cation arrangements within 2:1 layer-silicate interlayers depend on layer-charge magnitude and density. Low-charge smectite-group minerals have monolayer (~13.6 Å), bilayer (~17.7 Å), or pseudotrimolecular (21.7 Å) arrangements. Long-chain *n*-alkylammonium cations, such as octadecylammonium, form 25 to >30 Å paraffin-type arrangements (Figure 2)

https://doi.org/10.1346/CCMN.2014.0620407 Published online by Cambridge University Press

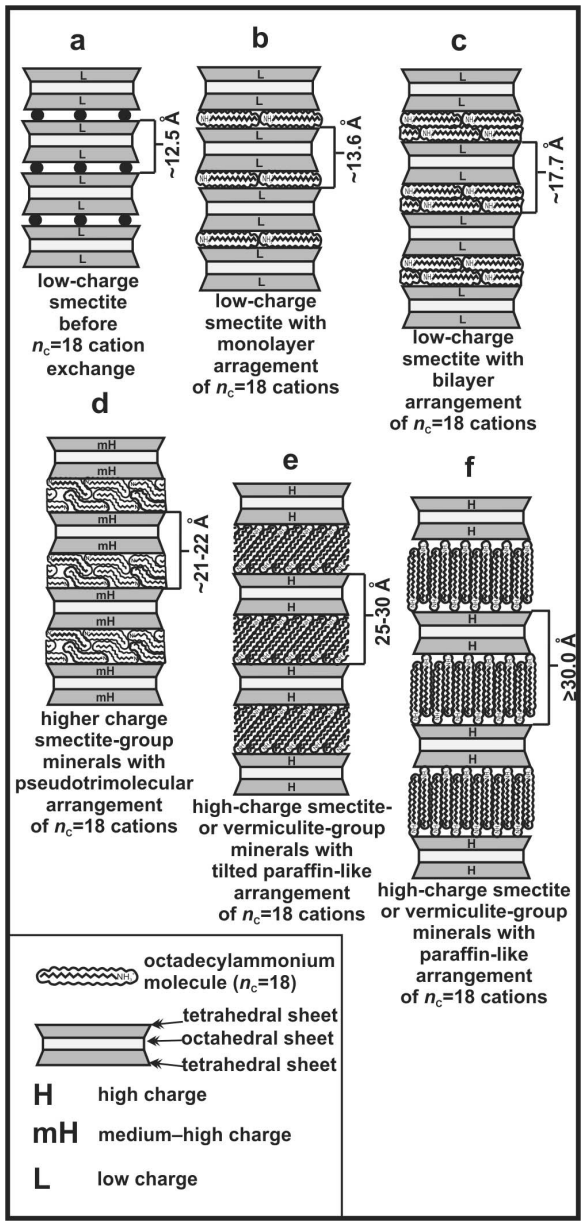

Figure 2. Schematic model showing smectite-group and vermiculite-group 2:1 layer silicates before and after treatment with octadecylammonium (n_C = 18) cations (not to scale): (a) low-charge smectite-group mineral; (b–c) low-charge smectite-group mineral with a monolayer (13.6 Å) and bilayer (17.7 Å) arrangement of the octadecylammonium cations; (d) high-charge smectite-group or vermiculite-group 2:1 layer silicates with a pseudotrimolecular (21–22 Å) arrangement of octadecylammonium cations; (g–f) paraffin-like arrangement of octadecylammonium cations with different tilt angles of the alkyl chains. Diagrams based on the original drawings of Lagaly and Weiss (1969, 1970c), Lagaly (1981), and Vali *et al.* (1994).

in high-charge smectite-group minerals, vermiculite-group minerals, expandable illite, or altered micas (Lagaly and Weiss, 1969, 1970a, 1970c; Lagaly, 1981, 1982). A pseudotrimolecular arrangement can form in 2:1 layer silicates with a layer charge of >0.4 eq/$O_{10}(OH)_2$ whereas paraffin-type orientations of the alkyl chain occur at interlayer charges >0.63 eq/$O_{10}(OH)_2$ (Lagaly, 1982; Malla and Douglas, 1987; Lagaly and Dekany, 2005). For a detailed summary of the theoretical background of the *n*-alkylammonium cation-exchange method and additional references see Sears *et al.* (1998) as well as Laird and Fleming (2008).

XRD and TEM

To prepare octadecylammonium cation-exchanged samples for XRD analysis, ~40 mg of freeze-dried clay material were placed in 1.5 mL polypropylene Eppendorf micro-test tubes (Eppendorf Canada Limited, Streetsville, ON, Canada) and dispersed in a 0.05 M solution of octadecylammonium hydrochloride (n_C = 18) (Acros Organics, Thermo Fisher Scientific, New Jersey, USA) and left in an oven at 65ºC for 24 h. This exchange procedure was repeated four times. The samples were washed thoroughly up to 20 times with 100% ethanol to remove excess alkylammonium salts. The washed clays were dispersed in ~1 mL of 100% ethanol and pipetted onto glass slides, dried at room temperature, and X-rayed. The XRD analyses were performed using a Siemens D5000 diffraction system equipped with a Sol-X solid-state detector with CoKα1,2 radiation in the Département des sciences de la Terre et de l'atmosphère of Université du Québec à Montréal (Québec, Canada). The following analytical conditions were used: operating voltage of 40 kV, beam current of 30 mA, step-size of 0.02º2θ, counting time of 2 s per step, 0.02 mm receiving slit, and scanning range of 1.75 to 55º2θ. After analyses the Co-Kα1,2 radiation was converted numerically into CuKα radiation and the background as well as the Kα2 signal were removed from the XRD patterns.

For HRTEM investigations the samples were embedded in Epon epoxy resin (Electron Microscopy Sciences, Hatfield, Pennsylvania, USA) (Figure 1: method 2). For this procedure, ~10–20 mg of freeze-dried clay samples were placed in 1.5 mL polypropylene Eppendorf micro-test tubes and dehydrated for 48 h by adding 100% acetone to remove adsorbed water. After centrifugation at 16060 × *g* for 15 min with an accuSpin Micro bench-top centrifuge (Fisher Scientific Company, Ottawa, ON, Canada), the supernatant was removed and the clay material dispersed in a mixture of 10% Epon resin and 90% acetone. These steps were repeated with mixtures containing 30%, 50%, 70%, and 100% resin. The dispersion of the material in the acetone resin mixtures was achieved through stirring and agitation using an electrical shaker. Each incubation step lasted 24 h and during that time the samples were placed on a rotating plate to ensure continuous agitation of the material. The resin-clay mixture was transferred into embedding molds after the fifth incubation step (100% Epon resin). After a

https://doi.org/10.1346/CCMN.2014.0620407 Published online by Cambridge University Press

settling time of 1−2 h the embedding molds (Electron Microscopy Sciences, Hatfield, PA, USA) were placed in an oven for 48 h at 65ºC. Ultrathin sections (~80 nm) were obtained from the polymerized resin blocks using a Reichert-Jung Ultracut E microtome (C. Reichert AG, Vienna, Austria) and transferred to 300-mesh copper TEM grids with carbon support film (Structure Probe, Inc. West Chester, Pennsylvania, USA).

The octadecylammonium cation-exchange treatment was carried out using a modified version of the procedure described by Vali and Hesse (1990). Each grid was placed face down in a 1.5 mL micro-test tube on the surface of the octadecylammonium cation solution diluted to 50% (0.025 M). The micro-test tubes were left for 20 min in an oven at 65ºC. The grids were removed from the tubes, held submerged in a Petri dish filled with 65ºC preheated distilled water and agitated gently for several minutes in order to remove excess alkylammonium solution and salts.

Some aliquots of the Upton and Otay montmorillonite were first treated with octadecylammonium cations and then embedded in Epon resin (Figure 1: method 1). These samples were treated in a 5-day cation-exchange reaction like those that were prepared for XRD analyses. An additional sample of Upton montmorillonite was only treated with octadecylammonium cations for 20 min, washed and embedded. The different treatment methods were chosen in order to compare possible differences in the expansion behavior caused by the different order of the treatment steps.

All samples were studied in bright-field illumination mode at an acceleration voltage of 200 kV with a Philips CM200-TEM at the Facility for Electron Microscopy Research (FEMR) of McGill University (Montreal, Canada). The TEM is equipped with a Gatan Ultrascan 1000 2k × 2k CCD Camera and an EDAX Genesis Energy-Dispersive X-Ray Spectroscopy system (EDS). The spherical aberration coefficient for the TEM is 1.2 mm. Lattice-fringe images were taken at Scherzer defocus (underfocus) conditions at magnifications of 59000−75000 (Vali *et al.*, 1991; Vali and Hesse, 1992). Lattice-fringe measurements were taken, when possible, on sets of lattice fringes. For *d* values of single bilayers, measurements were taken throughout the images on similar layers in order to obtain representative *d* values. The *d*-value measurements were taken using the graphics program *CorelDRAW*® X3 and calculated in Microsoft® *EXCEL*.

RESULTS AND DISCUSSION

Upton and Otay montmorillonite (<0.1 μm)

The incubation of the <0.1 μm grain-size fraction of Upton montmorillonite in octadecylammonium cations for 20 min and for 5 days resulted in similar XRD patterns. A sharp first-order reflection appeared at 5.02º2θ (17.58 Å) followed by integral reflections at 8.77 Å (002), 5.83 Å (003), 4.37 Å (004), 3.50 Å (005), 2.92 Å (006), and 1.95 Å (009) (Table 2).

The Otay montmorillonite <0.1 μm grain-size fraction exchanged with octadecylammonium cations showed a first-order reflection at 20.32 Å in the XRD pattern followed by nearly integral reflections at 10.39 Å (002), 6.98 Å (003), 5.44 Å (004), 4.36 Å (005), 3.54 Å (006), and 3.07 Å (007) (Table 2).

20 min octadecylammonium cation-exchange treatment of ultrathin sections after embedding and sectioning (method 2). Lattice-fringe images of ultrathin sections of Upton montmorillonite after treatment with octadecylammonium cations showed thick packets or ribbons of 2:1 layer-silicate sequences with a spacing ranging between 13 and 14 Å (Figure 3a). The spacings measured in the lattice-fringe images are different from those obtained from the XRD pattern of the octadecylammonium-treated sample. The 13−14 Å sequences suggest a monolayer arrangement of the octadecylammonium cations in the interlayer space whereas the first-order XRD reflection of 17.58 Å is typical for a bilayer arrangement (Figure 2b,c).

Lattice-fringe images of Otay montmorillonite ultrathin sections treated with octadecylammonium cations showed short sequences of two to five 2:1 silicate layers with a spacing between 13 and 14 Å (white half circles), highly expanded sequences of two to eight 2:1 silicate layers with spacing ranging between 26 and 45 Å (white diamonds), and sequences of 2:1 silicate layers containing both low (13 to 14 Å) and highly (26 to 45 Å)

Table 2. XRD peaks of the octadecylammonium cation-exchanged <0.1 μm grain-size fractions of Upton montmorillonite (UM) and Otay montmorillonite (OM).

Sample	Treatment	001 2θ / Å	002 2θ / Å	003 2θ / Å	004 2θ / Å	005 2θ / Å	006 2θ / Å	007 2θ / Å	009 2θ / Å
Upton	octadecylammonium cations for 20 min	5.02 / 17.58	10.08 / 8.77	15.18 / 5.83	20.30 / 4.37	25.42 / 3.50	30.54 / 2.92		46.44 / 1.95
Upton	octadecylammonium cations for 5 days	5.02 / 17.58	10.08 / 8.77	15.18 / 5.83	20.30 / 4.37	25.42 / 3.50	30.54 / 2.93		46.44 / 1.95
Otay	octadecylammonium cations for 20 min	4.34 / 20.32	8.49 / 10.39	12.66 / 6.98	16.28 / 5.44	20.34 / 4.36	25.13 / 3.54	28.97 / 3.08	

https://doi.org/10.1346/CCMN.2014.0620407 Published online by Cambridge University Press

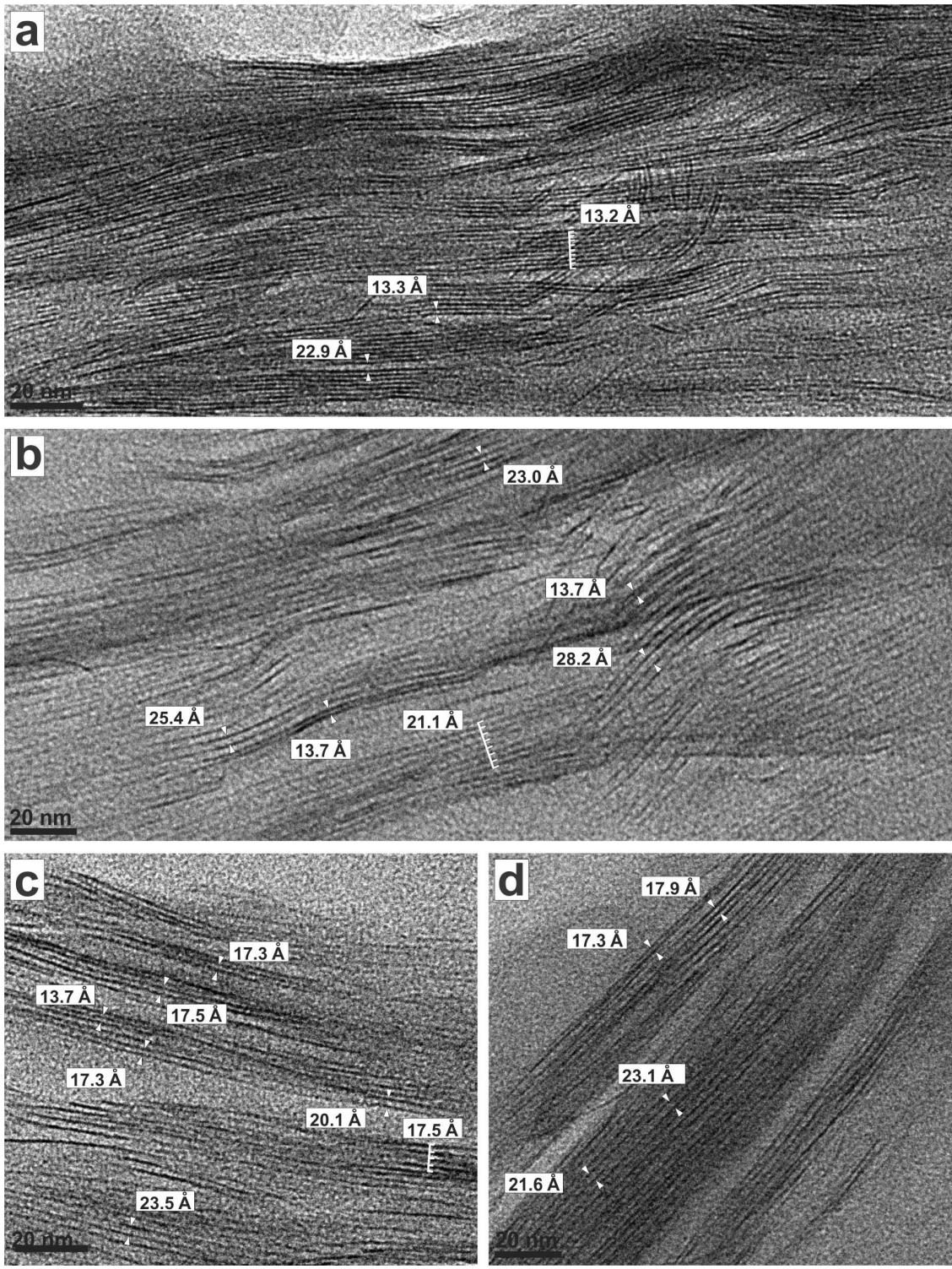

Figure 3. TEM lattice-fringe images of the ultrathin sections of Upton montmorillonite: (a) HRTEM image of an ultrathin section after treatment for 20 min with octadecylammonium cations (method 2) with sequences of silicate layers spacings of 13−14 Å; (b) lattice-fringe images of Upton montmorillonite treated for 20 min with octadecylammonium cations before embedding in resin (method 1). Most crystals are expanded significantly with spacings of between 21 and 26 Å. Some double layers or short sequences show 13−14 Å spacings; (c−d) Lattice-fringe images of Upton montmorillonite exchanged for 5 days with octadecylammonium cations before embedding (method 1). Most crystals show sequences with spacings of 21−25 Å and 17−18 Å. Some crystals have short sequences with 13 to 14 Å spacings.

https://doi.org/10.1346/CCMN.2014.0620407 Published online by Cambridge University Press

expanded interlayers in a random distribution (Figure 4a–e). Lattice-fringe images also showed the presence of short sequences composed of alternating low (13–14 Å) and highly (26–45 Å) expanded 2:1 silicate layers resembling a rectorite-like structure (Figure 4b,d,e: white star). The spacings measured using HRTEM contrast with the results obtained by XRD. The 20.32 Å spacing observed in the XRD pattern suggests a pseudotrimolecular arrangement of the octadecylammonium cations (Figure 2e). The 13–14 Å layers in lattice fringes have a monolayer structure while the highly expanded 26–45 Å sequences could be interpreted as a paraffin-type arrangement of octadecylammonium cations (Figure 2b,e,f).

20 min octadecylammonium cation-exchange treatment before embedding (method 1). Lattice-fringe images of Upton montmorillonite treated with octadecylammonium cations for 20 min before embedding mainly showed disrupted 2:1 silicate-layer sequences. The majority of the sequences consisted of highly expanded 2:1 silicate layers with spacings ranging between 21 and 26 Å (Figure 3b). Some sequences showed spacings as large as ~34 Å (not illustrated in any of the figures). Other 2:1 silicate layers showed expansions of 13–14 Å similar to the spacings observed in lattice-fringe images of the ultrathin sections treated with octadecylammonium cations after embedding.

Five days of octadecylammonium cation-exchange treatment before embedding (method 1). Lattice-fringe images of Upton montmorillonite treated for 5 days with octadecylammonium cations before embedding showed highly expanded sequences of 2:1 silicate layers with spacings of 21–25 Å, short sequences with spacings between 17 and 18 Å, and minor amounts of 2:1 silicate layers with 13–14 Å spacings (Figure 3c,d). Some highly expanded sequences reached spacings of up to 34 Å. The measured *d* values between 17 and 18 Å were in the same range of spacings obtained from the XRD analyses of the material exchanged with octadecylammonium cations (Table 2).

The Otay montmorillonite sample treated with octadecylammonium cations before embedding showed packets of highly expanded sequences of 2:1 silicate layers with spacings ranging between 20 and 26 Å (Figure 4f).

Synthetic fluorohectorite

Lattice-fringe images of ultrathin sections of the 0.4 eq/$O_{10}(OH)_2$ fluorohectorite treated with octadecylammonium cations after embedding and sectioning (method 2) showed both crystals with highly expanded 21–27 Å silicate layers and others with a spacing of 13–14 Å (Figure 5a,b). These structures occur, in many instances, within the same crystal (Figure 5c, d). They resemble a rectorite-like structure if they occur in an alternating manner (Figure 5d: white stars). Some of the 2:1 silicate layers changed their expansion behavior within one layer from a small spacing (13 to 14 Å) to a large expansion (21 to 27 Å) (Figure 5a,c,d: white arrows). Some highly expanded sequences reached spacings of up to 30 Å.

Lattice-fringe images of ultrathin sections of the 0.6 eq/$O_{10}(OH)_2$ fluorohectorite treated with octadecylammonium cations revealed the predominance of thick sequences of highly expanded 2:1 silicate layers with *d* values ranging between 21 and 27 Å (Figure 5e, f). Some layers reached spacings of up to 30 Å. In some cases, layers with 13–14 Å spacing occurred within these highly expanded sequences (Figure 5f).

Comparison between d values obtained from XRD and TEM treatment method 1 and 2

Upton montmorillonite exchanged with octadecylammonium cations showed a first-order reflection of 17.58 Å in XRD pattern. In TEM lattice-fringe images, the same exchanged material embedded in epoxy resin (method 1) showed disrupted and highly expanded packets of 2:1 silicate layers with spacings ranging from 21 to 34 Å. Similar highly expanded packets of 2:1 silicate layers were observed by Vali (1983) and Vali and Köster (1986) for Upton montmorillonite and hectorite (Hector, California) in lattice-fringe images despite the slightly different pre-treatment procedure. Those authors' samples were also saturated with Na before they were exchanged for only 3 h with octadecylammonium cations and embedded in epoxy resin (Table 3).

Otay montmorillonite from the present study prepared according to method 1 also showed highly expanded sequences of 2:1 silicate layers in lattice-fringe images (20–26 Å) (Figure 4f) but only 20.32 Å as a first-order XRD reflection (Table 3). Similar discrepancies between XRD peak maxima and measured stacking periodicities on HRTEM images were observed by Malla *et al.* (1993) for the montmorillonite samples SWy-1 and SAz-1 exchanged with dodecylammonium (n_C = 12) cations and embedded in Spurr resin. The XRD patterns showed first-order reflections of 17.70 Å while lattice-fringe images showed highly expanded packets ranging from 20 to 48 Å (compare column 3 and 4 for smectites in Table 3). The large expansion of the 2:1 silicate layers in the lattice-fringe images of material treated with *n*-alkylammonium cations before embedding (method 1) can be attributed to the intrusion of epoxy resin into the interlayer spaces that were already expanded by the intercalation of *n*-alkylammonium cations (Vali and Köster, 1986; Laird *et al.*, 1989b; Malla *et al.*, 1993).

Different expansion behaviors of smectite-group minerals can be observed if the samples are treated with *n*-alkylammonium cations after embedding and cutting of ultrathin sections (method 2). For example,

https://doi.org/10.1346/CCMN.2014.0620407 Published online by Cambridge University Press

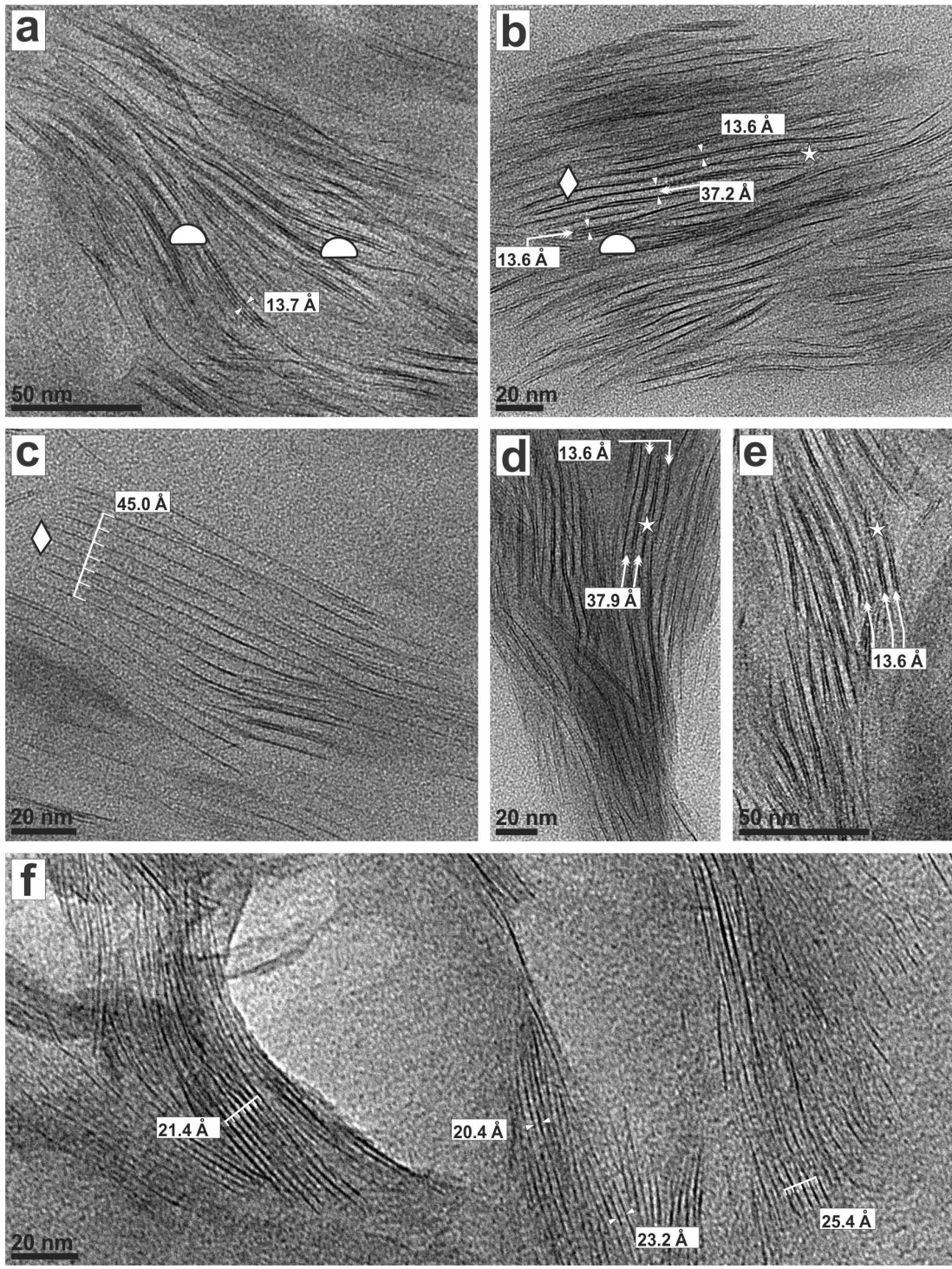

Figure 4. (a–e) HRTEM lattice-fringe images of Otay montmorillonite after treatment with octadecylammonium cations (method 2) showing the different expanded 2:1 silicate layer sequences. Short sequences of 2:1 silicate layers with *d* values of 13–14 Å (white half-circles in parts a and b). Sequences with highly expanded 26–45 Å silicate layers (white diamonds in parts b and c). Both structures may also occur within the same crystal (b,d,e). Some crystals also contain alternating highly expanded layers (26–45) and 13–14 Å layers which resemble rectorite-like structures (white stars in parts b, d, and e). (f) Lattice-fringe images of Otay montmorillonite treated with octadecylammonium cations before embedding in epoxy resin (method 1) showing the predominance of disrupted, highly expanded sequences of 2:1 silicate layers with 20–26 Å spacings. The different expansion behavior of the silicate layers which are due to interlayer-charge differences can only be observed in samples prepared according to method 2.

https://doi.org/10.1346/CCMN.2014.0620407 Published online by Cambridge University Press

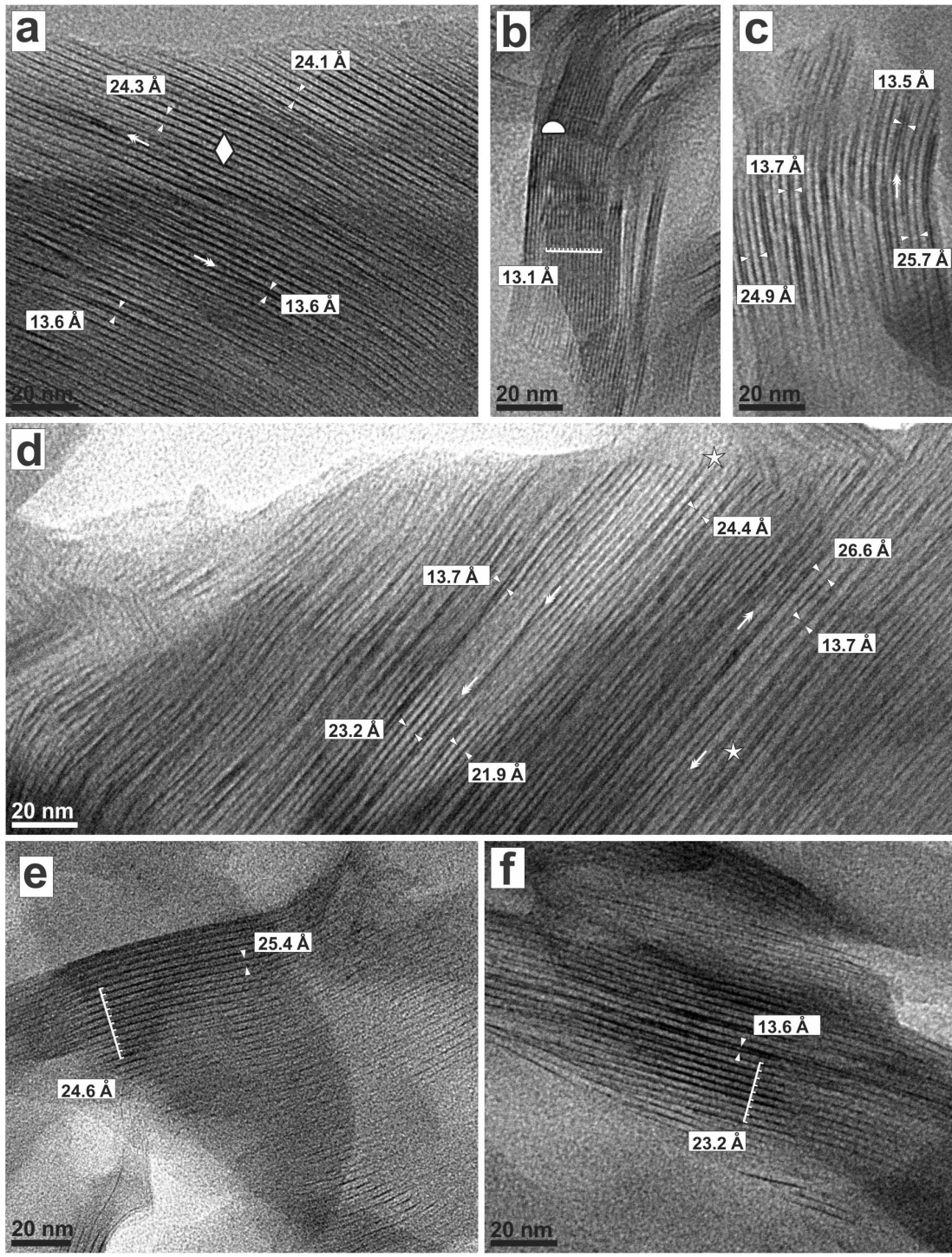

Figure 5. HRTEM lattice-fringe images of synthetic fluorohectorite samples with layer charges of 0.4 and 0.6 eq/$O_{10}(OH)_2$. The ultrathin sections of the of 0.4 eq/$O_{10}(OH)_2$ fluorohectorite treated according to method 2 reveal several different expanded structures: (a) large crystals with highly expanded 2:1 silicate layers with 24–25 Å spacings (white diamond). Some layers show expansions of 13–14 Å.(b) Crystals that only have layers with an expansion of 13–14 Å (white half circle). (c–d) Highly expanded silicate layers (21–27 Å) and 13–14 Å layers commonly occur within the same crystal. In many cases, the alternation of these layers generate short sequences resembling rectorite-like structures (white stars in d). The expansion behavior can also change laterally within the same silicate layer indicating a change in layer charge (white arrows in a, c, and d). (e–f) Lattice-fringe images of 0.6 eq/$O_{10}(OH)_2$ fluorohectorite show crystals with highly expanded silicate layers of between 23 and 26 Å. Some of these highly expanded sequences can contain 13–14 Å layers.

https://doi.org/10.1346/CCMN.2014.0620407 Published online by Cambridge University Press

Table 3. List of d values of smectite-group mineral samples after treatment with n-alkylammonium cations obtained from XRD analyses and TEM lattice-fringe measurements. Column 3 shows the spacings obtained from XRD analyses. Columns 4 and 5 list spacings from TEM lattice-fringe measurements. Values in column 4 were obtained from samples that were treated with n-alkylammonium cations before embedding in epoxy resin and the preparation of ultrathin sections (method 1). Values in column 5 are from samples that were treated with n-alkylammonium cations after embedding in epoxy resin and the preparation of ultrathin sections (method 2). The cation-exchange procedure was performed on ultrathin sections on the TEM grids.

1	2	3	4	5	6
		XRD	TEM		
Sample	Layer charge	n-alkylammonium cation exchange †(n_C = 18 for 5 days); ‡(n_C = 18 for 20 min); §(n_C = 18 for 2 days); *(n_C = 12 for 2 days)	n-alkylammonium cation exchange (method 1)	n-alkylammonium cation exchange (method 2)	Reference (grain-size fraction)
	eq/$O_{10}(OH)_2$	d_{001}	d_{001}	d_{001}	
Smectite-group minerals					
Upton montmorillonite (A.P.I. No. 25)	0.36[1] 0.38[2]	17.58 Å†	Majority 21–25 Å† and 17–18 Å†; max. ~31 Å; a few 13–14 Å	13–14 Å	Present study (<0.1 μm)
		17.58 Å‡	Majority 21–26 Å‡; a few 13–14 Å‡; max. ~34 Å		
		17.80 Å§	20–30 Å§		(Vali, 1983; Vali and Köster, 1986) (<0.6 μm)
Otay montmorillonite (A.P.I. No. 24)	0.38–0.60[2] 0.62[3];	20.32 Å†	20–26 Å†	2 kinds of layers: 13–14 Å; 26–45 Å	Present study (<0.1 μm)
Chisholm montmorillonite (A.P.I No. 21)	0.36[1]	19.70 Å§	~20 Å§		(Vali and Köster, 1986) (<0.6 μm)
SWy-1 Na-montmorillonite	0.21–0.37[4]; 0.34[5]	17.70 Å*	20–48 Å*		(Malla *et al.*, 1993)
		16.51 Å*	15–16 Å*		(Klimentidis and Mackinnon, 1986) (<2.0 μm)
SAz-1 Ca-montmorillonite	0.31–0.49[4]	17.70 Å*	20–44 Å*		(Malla *et al.*, 1993)
Hectorite, Hector, California	0.31[6]	17.30 Å§	20–34 Å§		(Vali and Köster, 1986) (<0.6 μm)
Fluorohectorite, synthetic	0.40[7]			2 kinds of layers: 13–14 Å; 21–27 Å (max. 30 Å)	Present study

Fluorohectorite, synthetic	0.60[8]			2 kinds of layers: majority 21–27 Å (max. 30 Å); a few 13-14 Å	this study
Smectite-group minerals (continued)		— §(n_C = 18 for 2 days) — d_{001}	d_{001}	d_{001}	
Nontronite, Hundsangen	0.39[9], 0.36[10]	22.00 Å§	22–25 Å§		
Nontronite SWa-1	0.50[11]			20–28 Å	(Vali and Köster, 1986) (<0.6 μm)
	0.54[12]				(Vali and Hesse, 1990)

[1] Vogt and Köster (1978); [2]Schultz (1969); [3]Hetzel and Doner (1993); [4]Malla and Douglas (1987a, 1987b); [5]Jaynes and Bigham (1987); [6]Ames *et al.* (1958); [7]Dr J. Breu (unpublished results); [8]Kalo *et al.* (2010); [9]Kerschreiter (1975); [10]Köster *et al.* (1999); [11]Bujdak *et al.* (1998); [12]Rozenson and Heller-Kallai (1976); (n_C = 18) = octadecylammonium cations; (n_C = 12) = dodecylammonium cations.

the treatment of ultrathin sections of Upton montmorillonite does not result in the large expansion of the silicate layers that was observed in lattice-fringe images of the same material treated with octadecylammonium cations before embedding and cutting (method 1). Lattice-fringe images showed thick sequences of 2:1 silicate layers with a uniform expansion of 13–14 Å (Figure 3a).

Lattice-fringe images of other smectite-group minerals such as Otay montmorillonite or synthetic fluorohectorite showed sequences of highly expanded 2:1 silicate layers (26–45 Å) and sequences with an expansion of 13–14 Å (Figures 4a–e, 5a–d; Table 3, column 5). Both layer types also occurred frequently within the same crystal in short alternating sequences that resemble rectorite-like structures (Figures 4b,d,e, 5c,d: white stars). Instead of containing non-expanded ~10 Å double layers as in rectorite, however, the double layers in the Otay montmorillonite and the fluorohectorite are silicate layers with a spacing of 13–14 Å.

What is the reason for these differences? Why did Upton montmorillonite only show sequences of 13–14 Å in lattice-fringe images while Otay montmorillonite showed both 13–14 Å and highly expanded structures of 26–45 Å? What caused the difference in the spacings obtained from XRD analyses and those measured in HRTEM lattice-fringe images?

The 13–14 Å silicate layers in lattice-fringe images (method 2)

A possible reason for the discrepancy between spacings obtained from XRD for Upton montmorillonite (17.58 Å) and those measured in lattice-fringe images (13–14 Å and 26–45 Å) was the different treatment methods (methods 1 and 2). The expansion behavior of smectite-group minerals in ultrathin sections treated with octadecylammonium cations depends essentially on the level of the layer charges. Based on XRD analyses, the transition from a monolayer (~13.6 Å) to a bilayer arrangement is achieved if the layer charge of the 2:1 layer silicate is >0.24/$O_{10}(OH)_2$ (Maes *et al.*, 1979).

Upton montmorillonite has an average interlayer charge of 0.36/$O_{10}(OH)_2$ and the bilayer arrangement of octadecylammonium cations (17.58 Å) was achieved both in a 20 min and a 5-day exchange process for XRD samples (Table 2). The evaluation of the XRD patterns alone would suggest that the time period of the exchange treatment does not have an influence on the arrangement of octadecylammonium cations in the interlayer space. However, evaluation of the HRTEM lattice-fringe images of the sample treated for 20 min and for 5 days with octadecylammonium cations before the embedding (method 1) suggested that time did indeed play a role. Both samples showed the predominance of disrupted highly expanded sequences with 21 to 34 Å spacings that were originally 17–18 Å structures with bilayer arrangement before the intrusion of resin into the

https://doi.org/10.1346/CCMN.2014.0620407 Published online by Cambridge University Press

interlayer space during the embedding. The '20 min' sample (method 1) also contains minor amounts of double layers and short sequences with an expansion of 13 to 14 Å (Figure 3b, Table 3).

The sample exchanged for 5 days (method 1), in addition to highly expanded sequences, also showed silicate layers with spacings of 17−18 Å and only very few silicate layers with expansions of 13−14 Å (Figure 3c,d). The silicate layers with spacings of 13−14 Å and 17−18 Å in both the '20 min' and the '5 day' samples did not experience additional intrusion of the embedding resin. The presence of the 13−14 Å layers in the lattice-fringe images of the '20 min' sample suggests that the time of 20 min was not sufficiently long to completely form a bilayer arrangement in the very low-charge 2:1 silicate-layer sequences. However, a bilayer arrangement of the octadecylammonium cations in the lower-charge interlayers was achieved after a 5 day exchange period, which is shown by the 17−18 Å layers in the lattice-fringe images (Figure 3c,d). The minor amount of 13−14 Å layers that were still observable in lattice-fringe images of the '5 day' sample probably originated from silicate layers with a charge of $<0.24/O_{10}(OH)_2$ as a transition from monolayer to bilayer is only achieved by charges $>0.24/O_{10}(OH)_2$ (Maes *et al.*, 1979).

The short time period of 20 min for the octadecylammonium cation-exchange treatment of ultrathin sections (method 2) of Upton montmorillonite could have been one reason why lattice-fringe images only showed sequences with a spacing of 13 to 14 Å (Figure 3a). The layer charges were simply not high enough to achieve greater expansion during the short exchange period. The possibility that a bilayer arrangement (17−18 Å) of the octadecylammonium cations could have been achieved if the exchange time for method 2 was extended to 5 days was tested. Large crystals of octadecylammonium salts form everywhere on the TEM copper grid during this long exchange time and cover the ultrathin sections of the clay minerals, however, which makes it impossible to investigate the layer structure in TEM. An intensive washing procedure with ethanol in order to remove the octadecylammonium salts as was done for the XRD sample materials was not an option because the ethanol would have destroyed the epoxy ultrathin sections that contain the clay minerals on the TEM grids. The gentle washing of the TEM grids with preheated distilled water (method 2) in a Petri dish works reasonably well for removing excess octadecylammonium solution from the surface of the ultrathin sections that were exchanged for 20 min but not for ultrathin sections on TEM grids that were exchanged for 5 days.

Exchange kinetics may play a role for samples prepared according to method 2 but the interlayer charges also have an influence on the expansion behavior. While Upton montmorillonite only shows sequences with 13–14 Å layers, Otay montmorillonite ultrathin sections treated with octadecylammonium cations (method 2) showed both highly expanded silicate layers (26−45 Å) and layers with spacings of 13−14 Å within the same crystal (Figure 4a−e). Otay montmorillonite is a smectite-group mineral with a heterogeneous interlayer charge distribution ranging between 0.38 and 0.62 $eq/O_{10}(OH)_2$ (Schultz, 1969; Hetzel and Doner, 1993). The occurrence of sequences that contain both layer types illustrates the presence of differently charged 2:1 silicate layers within the same crystal.

The same material treated with octadecylammonium cations before the resin impregnation, however, showed lattice-fringe images of highly expanded sequences of 2:1 silicate layers with spacings ranging from 20 to 26 Å (Figure 4f). No significant spacing differences (interlayer-charge heterogeneities), either laterally or in the stacking direction, were observed in Otay montmorillonite crystals prepared using method 1. The interlayer-charge heterogeneities that are revealed in lattice-fringe images from octadecylammonium cation-exchanged ultrathin sections (method 2) cannot be seen in these images (Figure 4a−e,f).

The lattice-fringe images from the different embedding and octadecylammonium cation treatment methods for the Upton and Otay montmorillonite as well as the data from Vali and Köster (1986) and Malla *et al.* (1993) confirmed that smectite-group minerals treated with *n*-alkylammonium cations before embedding in epoxy resin (method 1) will appear mainly as highly expanded sequences of 2:1 silicate layers, due to the additional incorporation of resin molecules into the interlayer space (Table 3, columns 2 and 4). The evaluation of such lattice-fringe images would, therefore, lead to an incorrect interpretation of the interlayer charge properties of members of this 2:1 layer silicate group, if the effects of sample treatment were not taken into consideration.

The highly expanded 2:1 silicate layers in lattice-fringe images (method 2)

The question that has to be answered next is the discrepancy between the relatively large expansions of 26−45 Å observed in lattice-fringe images of the Otay montmorillonite prepared according to method 2 and the spacing of 20.32 Å obtained from the XRD pattern (Table 2, Figure 4b−e; Table 3, columns 3, 5). The difference in the values can be explained by the different preparation techniques. In method 2, the clay minerals were embedded without pre-treatment (Figure 1) and therefore the intrusion of epoxy resin into the interlayer space of the Otay montmorillonite silicate layers sequences was less likely, which contrasts with the smectite-group minerals that were treated with octadecylammonium cations before embedding (method 1).

Observations by TEM showed that clay-mineral aggregates were engulfed by resin during the embedding process (method 2) and only some clay minerals on the outsides of the particles were affected by resin

https://doi.org/10.1346/CCMN.2014.0620407 Published online by Cambridge University Press

infiltration, not crystals in the interior parts of larger crystal aggregates. During the treatment procedure of the ultrathin sections on the TEM grids, the exchangeable inorganic interlayer cations are replaced by *n*-alkylammonium cations which expand the 2:1 clay-mineral structures according to their layer charges. After this exchange reaction, additional pairs of *n*-alkylammonium cations can enter the interlayer space and are held there through van der Waals interactions (Lee and Kim, 2002; He *et al.*, 2004). The gentle washing process of the TEM grid with the ultrathin sections in preheated distilled water did not completely remove all excess *n*-alkylammonium molecules from the interlayer space. The use of ethanol for the washing was not an option for carbon-coated TEM grids that contain ultrathin sections of clay minerals in Epon epoxy resin, because the ethanol would destroy the carbon film and the epoxy resin.

Additional incorporation of *n*-alkylammonium cations into the interlayers of 2:1 silicate layers holding a certain threshold interlayer charge could be a reasonable explanation for the observed high expansion. This conclusion was supported by a study of Lee and Kim (2002) who investigated the effect of different concentrations of hexadecyltrimethylammonium (HDTMA) solutions on the expansion behavior of smectite-group minerals. The XRD patterns of their study showed first-order reflections of 27.6 and 40.5 Å for smectite-group minerals treated with a 0.01 M HDTMA solution that had a concentration equivalent to 1.5−2.5 times the cation exchange capacity (CEC) of the sample (104.3 meq/100 g). Additional incorporation of HDTMA molecules in the interlayer space and subsequent expansion up to 40 Å occurs through hydrophobic bonding if the alkylammonium molecule concentration increases beyond the CEC of the material (figures 2a, 10d of Lee and Kim, 2002).

Otay montmorillonite has a CEC of 121.0 meq/100 g (Maes and Cremers, 1977). The octadecylammonium hydrochloride solution used in the present study had a concentration of 0.025 M. The highest concentration of HDTMA used by Lee and Kim (2002) was close to 0.01 M and caused interlayer expansions of >40 Å. This concentration was still 0.015 M less than the concentration of the octadecylammonium solution (0.025 M) used in the present study. In the light of these results, the high concentration of the exchange solution in the present study probably caused the additional incorporation of octadecylammonium molecules into the interlayer space, generating the highly expanded (26−45 Å) 2:1 silicate layers. The arrangement of the octadecylammonium cations in the interlayer space is not known. They may be aligned in a dense paraffin-like arrangement in double layers (Lagaly, 1981; He *et al.*, 2004) or in a less dense irregular paraffin-type configuration as proposed by Lee and Kim (2002) (Figure 6b,c).

The question now arises as to why the XRD pattern of the octadecylammonium cation-exchanged Otay montmorillonite did not show these large expansions that were described for the smectite-group minerals used in the study of Lee and Kim (2002)? The difference was due to the different washing procedures used by Lee and Kim and in the present study. Their samples were washed only once with distilled water, whereas the octadecylammonium cation-exchanged samples of this study were washed up to 20 times with 100% ethanol before XRD analyses with the purpose of removing the excess *n*-alkylammonium molecules. On the other side, the gentle washing procedure of the TEM grids with the ultrathin sections after the octadecylammonium exchange treatment (method 2) in preheated distilled water, as used in this study, was indeed comparable to the "one-time" washing procedure of Lee and Kim (2002). This, however, was not sufficient to remove all excess *n*-alkylammonium molecules from the interlayer space and led to the observed highly expanded 2:1 silicate layers.

These findings showed once again that the arrangement of the alkylammonium cations within the 2:1 layer silicate interlayers depends upon the magnitude of the layer charge, the charge density, the concentration of the exchange solution, and the washing procedure (Lagaly and Weiss, 1969, 1970c; Lagaly, 1981, 1994; Lee and Kim, 2002).

As little about the washing procedure of the TEM grids with the ultrathin sections in preheated distilled water can be changed, future studies should test whether the excess incorporation of alkylammonium cations into the interlayer space of clay minerals prepared according to method 2 could be prevented by using lower concentrations of octadecylammonium cation exchange solutions. The solutions that should be tested in future studies should have concentrations of 0.01 M, 0.005 M, 0.0025 M, and 0.0001 M or even lower. Ultrathin sections (microtome sections) of one higher-charge smectite-group mineral, *e.g.* Otay montmorillonite, should be treated with these exchange-solution concentrations according to method 2. Lattice-fringe images of these samples will then show how the interlayer spacing is influenced by the concentration of the octadecylammonium exchange solution.

At what interlayer-charge threshold does the additional incorporation of n-alkylammonium cations in the interlayer space of smectite-group minerals occur?

The average interlayer charge for Upton montmorillonite is 0.36 eq/$O_{10}(OH)_2$ (Table 3). Lattice-fringe images of this sample showed only thick sequences with spacings of 13−14 Å. In contrast, the interlayer charges for Otay montmorillonite range from 0.38 to 0.62 eq/$O_{10}(OH)_2$ which is reflected in the different spacings observed in the lattice-fringe images (Figure 4b−e, Table 3). The minimum charge of 0.38 eq/$O_{10}(OH)_2$ probably corresponded to the limit for the 13−14 Å expansion.

Synthetically produced fluorohectorite with known interlayer charges was chosen in order to estimate the

https://doi.org/10.1346/CCMN.2014.0620407 Published online by Cambridge University Press

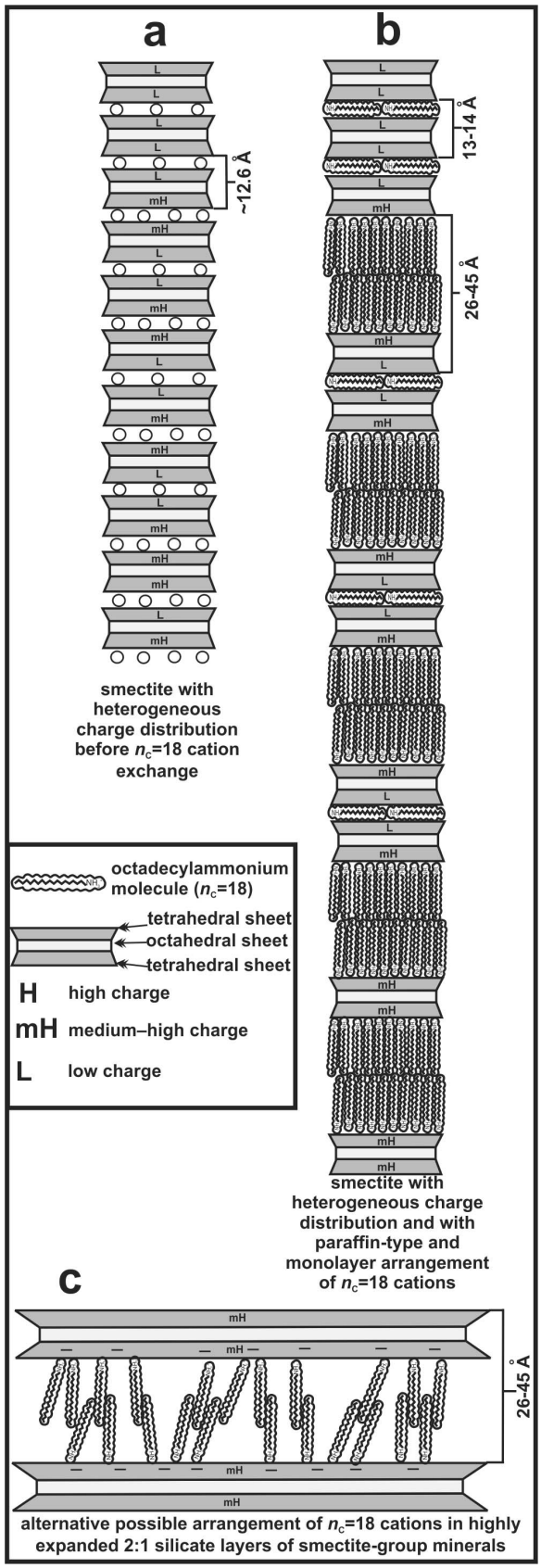

charge at which smectite 2:1 silicate layers in ultrathin sections showed large expansions after the treatment with octadecylammonium cations. Lattice-fringe images of the 0.4 eq/$O_{10}(OH)_2$ fluorohectorite also showed crystals both with highly expanded (21–30 Å) and less expanded (13–14 Å) 2:1 silicate layers (Figure 5a,b). Numerous fluorohectorite (0.4 eq/$O_{10}(OH)_2$) crystals also have rectorite-like sequences with alternating highly expanded 2:1 silicate layers (21–27 Å) and 13–14 Å layers (Figure 5c,d). The occurrence of such rectorite-like sequences was assumed by Breu *et al.* (2001) in a synthetic fluorohectorite with an average interlayer charge of 0.5 eq/$O_{10}(OH)_2$. The XRD patterns of the fluorohectorite (0.5 eq/$O_{10}(OH)_2$) treated with *n*-alkylammonium cations suggest a certain amount of regular interstratification of an R1-ordered structure containing monolayers and bilayers of *n*-alkylammonium cations (figure 10 in Breu *et al*., 2001).

The expansion behavior of the 0.4 eq/$O_{10}(OH)_2$ fluorohectorite crystallites suggested that not all crystals have the same interlayer-charge values. The charge values even differ within the same crystal, as shown by sequences containing both 13–14 Å and highly expanded 2:1 layers which are similar to the Otay montmorillonite. Therefore, the interlayer charge of 0.4 eq/$O_{10}(OH)_2$ for the fluorohectorite must be interpreted as an average value.

The proportion of highly expanded sequences of 2:1 silicate layers increases in lattice-fringe images of smectite-group minerals if the interlayer charge increases beyond 0.4 eq/$O_{10}(OH)_2$ as observed in images of the more highly charged fluorohectorite (0.6 eq/$O_{10}(OH)_2$). It showed crystals with highly expanded 2:1 silicate layers (Figure 5e, f). Some silicate layers with a monolayer arrangement (13–14 Å) also occurred within these sequences, but less frequently than in the lower-charge fluorohectorite (0.4 eq/$O_{10}(OH)_2$) (Figure 5f). These observations showed that even high-charge smectite-group minerals still contain some 2:1 silicate layers with low interlayer charges of <0.4 eq/$O_{10}(OH)_2$.

From the expansion behavior of the synthetic fluorohectorite, the Upton montmorillonite, and the

Figure 6. Models showing a smectite-group mineral with heterogeneous charge distribution before (a) and after (b) treatment with octadecylammonium cations (not to scale). This model illustrates the observations made in lattice-fringe images of Otay Montmorillonite and synthetic fluorohectorite (method 2). The 2:1 silicate layers with spacings of 13–14 Å are interpreted to have a monolayer arrangement of the octadecylammonium cations. The sequences with highly expanded 2:1 silicate layers can have a double-layer paraffin-like arrangement or may form some sort of irregular arrangement of the octadecylammonium cations as shown in model (c) (Lee and Kim, 2002). Diagrams (a) and (b) are modifications of original drawings by Lagaly and Weiss (1969, 1970a, 1970b, 1970c), Lagaly (1981), and Vali *et al*. (1994).

https://doi.org/10.1346/CCMN.2014.0620407 Published online by Cambridge University Press

Otay montmorillonite, the critical interlayer charge at which the silicate layers become highly expanded 2:1 silicate layers in the ultrathin sections is probably ~0.40 eq/$O_{10}(OH)_2$ with a minimum value of 0.38 eq/$O_{10}(OH)_2$ which is the lower value of the interlayer-charge range of the Otay montmorillonite (Table 3).

The fact that the Upton montmorillonite consists of sequences of 13–14 Å silicate layers in lattice-fringe images suggests that the layer charges are below the threshold of 0.38–0.40 eq/$O_{10}(OH)_2$ in order to develop expansions as in Otay montmorillonite or fluorohectorite.

The treatment of smectite-group minerals with octadecylammonium cations after preparation of the ultrathin sections (method 2) not only prevented disintegration of the primary arrangement of layers and additional expansion from infiltration of resin into the alkylammonium-expanded interlayer space of 2:1 layer silicates as suggested by Sears *et al.* (1998), it also allowed the distinction between differently charged 2:1 silicate layers within the same crystal. This treatment method illustrated well the differences in interlayer charges from layer to layer within the crystals. It made charge heterogeneities visible that occur within the same 2:1 silicate layer (Figure 5c,d: white arrows).

Reference samples vs. sample AD-D50 2035 m

Lattice-fringe images of the octadecylammonium cation-exchanged <0.1 μm size fraction of sample AD-D50 (2035 m) showed expanded structures of smectite-group minerals that are similar to those observed in lattice-fringe images of Otay montmorillonite and the synthetic fluorohectorite. The sample contained both smectite crystals that have highly expanded 2:1 silicate layers (white diamonds) ranging from 22 to 27 Å (maximum values up to 33 Å) and short sequences of silicate layers with an expansion between 13 and 14 Å (white half circles, Figure 7a,b). Both layer types occurred within the same crystal in random distribution but could also be observed as short rectorite-like sequences (Figure 7b). Minor amounts of illite packets (I) with 3–6 non-expanded ~10 Å layers also occur between smectite-group minerals (Figure 7a).

The observations made in lattice-fringe images from Otay montmorillonite, the synthetic fluorohectorite, and the sample AD-D50 (2035 m) suggest that crystals of smectite-group minerals may have, like rectorite, polar 2:1 silicate layers (Lagaly, 1979; Ahn and Peacor, 1986; Güven, 1991; Vali *et al.*, 1994). In rectorite, one of the tetrahedral sheets in the 2:1 silicate layers has a low charge and one a high charge. The low-charge layers in rectorite have a beidellite-like composition. Beidellite is a dioctahedral smectite-group mineral in which the majority of the interlayer charges originate from the tetrahedral sheets due to isomorphous substitution of Si^{4+} by Al^{3+}. The interlayer charges in the dioctahedral smectite mineral, montmorillonite, however, originates mainly from isomorphous substitution of trivalent (Al^{3+}, Fe^{3+}) by divalent cations (Fe^{2+}, Mg^{2+}) in the octahedral sheet. This charge can increase by reduction of Fe^{3+} to Fe^{2+} or decrease by oxidation of Fe^{2+} to Fe^{3+}. The synthetic fluorohectorite is a trioctahedral smectite in which the charge originates from the octahedral sheet due to isomorphous substitution of Mg^{2+} by Li^{+}. The rectorite-like appearance of 2:1 silicate layers in lattice-fringe images of Otay montmorillonite and synthetic fluorohectorite is, therefore, probably due to the heterogeneity of the occupancy in the octahedral sheets which causes a dissymmetry of the charges on the basal surfaces (interlayers) of the 2:1 silicate layers.

The fact that smectite-group minerals show rectorite-like expansion behavior in lattice-fringe images is an important finding for the characterization of clay-mineral assemblages that were previously interpreted to contain mixed-layer illite-smectite clay minerals (*e.g.* Abid *et al.*, 2004).

Rectorite-like, R1-ordered I-S structures, for example, were described from lattice-fringe images in studies by Vali *et al.* (1993) (their figure 4a–c), Sears *et al.* (1998) (their figure 6b), and Sears (2001). A reevaluation of the lattice-fringe images from those studies in light of present findings concluded that many of those R1-ordered structures are in fact smectite-group crystals with short sequences of alternating low-charge and high-charge silicate layers rather than I-S phases with expanded smectite layers and non-expanded (10 Å) illite double layers. They are smectite crystals with charge heterogeneities in the tetrahedral or octahedral sheets that cause a rectorite-like expansion behavior.

SUMMARY AND CONCLUSIONS

Alkylammonium cation exchange on ultrathin sections of smectite-group minerals and their subsequent examination using HRTEM can reveal layer-to-layer charge heterogeneities within crystals or even within the same 2:1 silicate layer. The treatment of the ultrathin sections with octadecylammonium cations after embedding in epoxy resin (method 2) made charge-density heterogeneities visible that could not be observed if the samples were treated with octadecylammonium cations before embedding (method 1). Treatment of the smectite-group minerals with octadecylammonium cations before resin impregnation expanded the 2:1 silicate layers and facilitated the intrusion of embedding resin into the interlayer space. This led to additional expansion and layer-sequence disintegration. Such charge heterogeneities within single smectite crystals, revealed by HRTEM imaging of ultrathin sections (method 2), were not revealed in XRD patterns.

The treatment of smectite-group minerals with octadecylammonium cations after ultrathin-section preparation (method 2) prevented disintegration of the primary layer arrangement and the additional expansion

https://doi.org/10.1346/CCMN.2014.0620407 Published online by Cambridge University Press

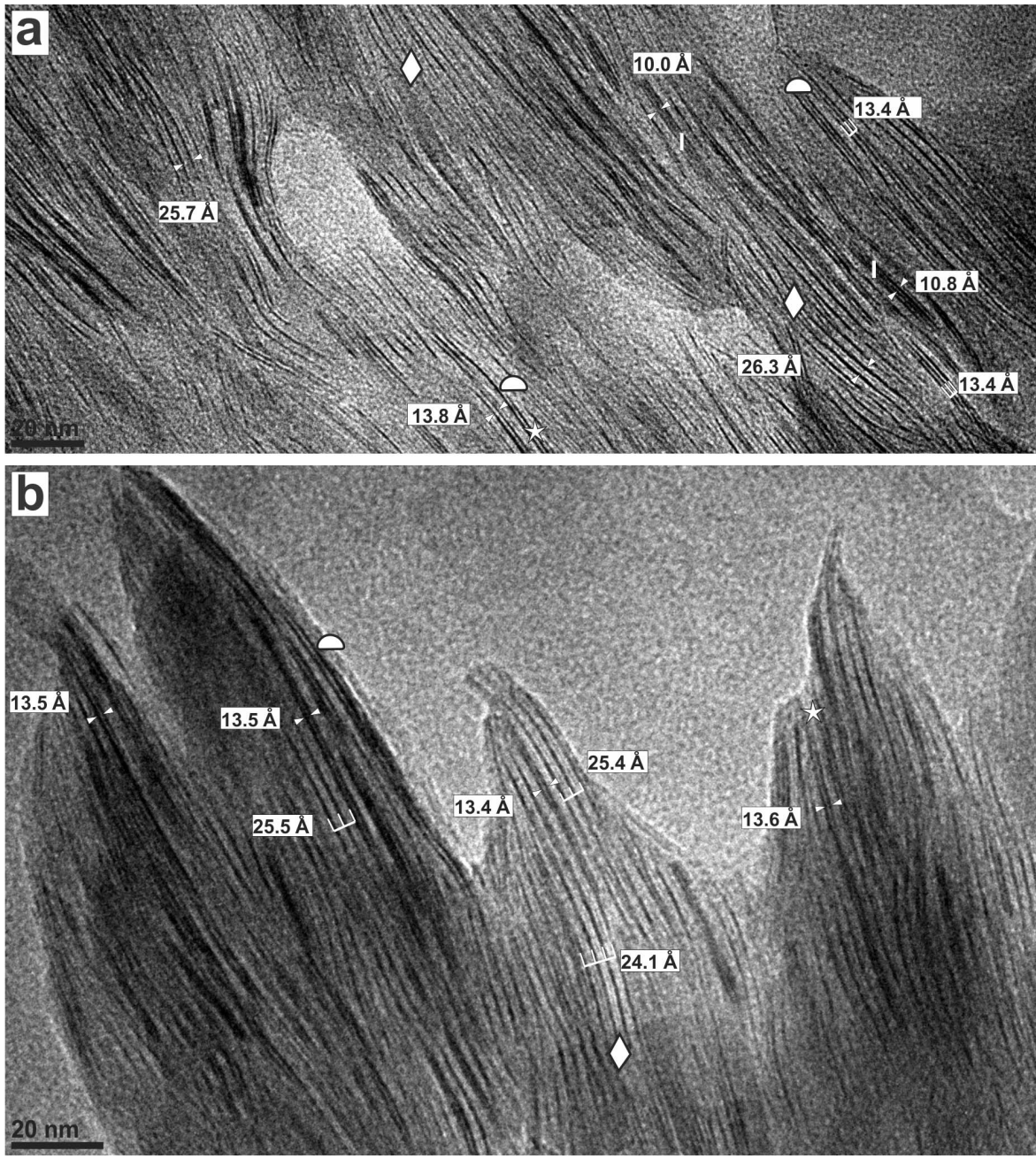

Figure 7. HRTEM lattice-fringe images of the octadecylammonium-exchanged <0.1 μm size fraction of sample AD D-50 (2035 m) showing smectite crystal aggregates with an expansion behavior that is similar to those observed in Otay montmorillonite and synthetic fluorohectorite. (a–b) Sequences of highly expanded (white diamonds) 2:1 silicate layers of smectite phases with 22–27 Å spacings. Sequences of low-charge smectite layers (13–14 Å) occur as separate phases or within high-charge smectite crystals (white half circles). Alternating low-charge and high-charge layers (white stars). Note the presence of minor amounts of authigenic illite (I) with spacings of 10–11 Å in image (a) that grow between the smectite-group mineral crystals.

due to resin infiltration into alkylammonium-expanded interlayers.

Smectite-group minerals with layer charges <0.38 eq/$O_{10}(OH)_2$ had spacings of 13–14 Å in lattice-fringe images, while silicate layers with >0.38 eq/$O_{10}(OH)_2$ showed spacings between 26 and 45 Å. Smectite crystals can also contain short sequences of highly-expanded (higher-charge) silicate layers that alternate with 13–14 Å silicate layers (lower charge) and resemble rectorite-like structures. This demonstrates that smectite-group minerals, similar to rectorite, may have alternating low- and high-charge 2:1 silicate layers. This finding is

https://doi.org/10.1346/CCMN.2014.0620407 Published online by Cambridge University Press

important for a correct interpretation of lattice-fringe images of clay-mineral assemblages that were previously thought to contain mixed-layer illite-smectite minerals.

Knowledge of the expansion behavior of 2:1 layer silicates, such as smectite-group minerals with a range of layer charge, can be used to distinguish the minerals in the clay-mineral assemblages from argillaceous rocks of sedimentary basins, soils, or in hydrothermal alteration zones. For example, smaller crystallites of vermiculite with no non-expanded and only highly expanded silicate layers are difficult to differentiate in clay-mineral assemblages from high-charge smectite-group minerals due to their similarity in lattice-fringe images. However, high-charge smectite-group crystals might also contain lower-charge 2:1 silicate layers due to charge heterogeneities. Thus, the existence of 13−14 Å layers within a highly expanded 2:1 silicate layer sequence indicates a high-charge smectite-group mineral with some low-charge layers. In contrast, unexpanded 2:1 silicate layers in vermiculite crystals with 9.3−10.5 Å spacings can be distinguished easily from the 13−14 Å layers that can occur in high-charge smectite-group minerals.

The results of this study also suggest that the discrepancies between *d* values measured in lattice-fringe images and those obtained from XRD analyses are related to HRTEM and XRD sample-preparation methods. Highly-expanded 2:1 silicate layers observed in lattice-fringe images of high-charge smectite-group minerals are caused by additional *n*-alkylammonium cations incorporated into the interlayers.

REFERENCES

Abid, I.A., Hesse, R., and Harper, J.D. (2004) Variations in mixed-layer illite/smectite diagenesis in the rift and post-rift sediments of the Jeanne d'Arc Basin, Grand Banks offshore Newfoundland, Canada. *Canadian Journal of Earth Sciences*, **41**, 401−429.

Ahn, J.H. and Peacor, D.R. (1986) Transmission electron-microscope data for rectorite − Implication for the origin and structure of fundamental particles. *Clays and Clay Minerals*, **34**, 180−186.

Breu, J., Seidl, W., Stoll, A.J., Lange, K.G., and Probst, T.U. (2001) Charge homogeneity in synthetic fluorohectorite. *Chemistry of Materials*, **13**, 4213−4220.

Brindley, G.W. (1966) Ethylene glycol and glycerol complexes of smectites and vermiculites. *Clays and Clay Minerals*, **6**, 237−260.

Cetin, K. and Huff, W.D. (1995) Characterization of untreated and alkylammonium ion-exchanged illite/smectite by high-resolution transmission electron-microscopy. *Clays and Clay Minerals*, **43**, 337−345.

C-NLOPB Schedule of Wells (2007) Well 44, Adolphus D-50, http://www.cnlopb.ca/well_alpha.shtml (accessed 24 June 2013)

Eberhart, J.P. and Triki, R. (1972) Method for obtaining thin sections of clay-minerals − Application to investigation of mixed-layer clay-minerals. *Journal of Microscopy*, **15**, 111−120.

Elsass, F., Chenu, C. and Tessier, D. (2008) Transmission electron microscopy for soil samples: preparation methods and use. Pp. 235−267 in: *Methods of Soil Analysis. Part 5. Mineralogical Methods* (A.L. Ulery and L.R. Drees, editors). Soil Science Society of America, Madison, Wisconsin, USA.

Ghabru, S.K., Mermut, A.R., and Starnaud, R.J. (1989) Layer-charge and cation-exchange characteristics of vermiculite (weathered biotite) isolated from a Gray Luvisol in north-eastern Saskatchewan. *Clays and Clay Minerals*, **37**, 164−172.

Graf von Reichenbach, H.G., Wachsmuth, H., and Marcks, C. (1988) Observations at the mica-vermiculite interface with HRTEM. *Colloid and Polymer Science*, **266**, 652−656.

Güven, N. (1991) On a definition of illite/smectite mixed-layer. *Clays and Clay Minerals*, **39**, 661−662.

He, H., Frost, R.L., Deng, F., Zhu, J., Wen, X., and Yuan, P. (2004) Conformation of surfactant molecules in the interlayer of montmorillonite studied by ^{13}C MAS NMR. *Clays and Clay Minerals*, **52**, 350−356.

Hetzel, F. and Doner, H.E. (1993) Some colloidal properties of beidellite − comparison with low and high charge montmorillonites. *Clays and Clay Minerals*, **41**, 453−460.

Lagaly, G. (1979) Layer charge of regular interstratified 2:1 clay minerals. *Clays and Clay Minerals*, **27**, 1−10.

Lagaly, G. (1981) Characterization of clays by organic-compounds. *Clay Minerals*, **16**, 1−21.

Lagaly, G. (1982) Layer charge heterogeneity in vermiculites. *Clays and Clay Minerals*, **30**, 215−222.

Lagaly, G. (1994) Layer charge determination by alkylammonium ions. Pp. 1−46 in: *Layer Charge Characteristics of 2:1 Clay Minerals* (A. Mermut, editor). CMS Workshop Lectures, **6**, The Clay Minerals Society, Boulder, Colorado, USA.

Lagaly, G. and Dekany, I. (2005) Adsorption on hydrophobized surfaces: Clusters and self-organization. *Advances in Colloid and Interface Science*, **114**, 189−204.

Lagaly, G. and Weiss, A. (1969) Determination of layer charge in mica-type layer silicates. *Proceedings of the International Clay Conference*, **1**, 61−80.

Lagaly, G. and Weiss, A. (1970a) Inhomogeneous charge distribution in mica-type layer silicates. Pp. 179−187 in: *Reunión Hispano-Belga de Minerales de la Arcilla* (L. Heller, editor). Consejo Cuperior de Investigaciones Cientificas, Madrid.

Lagaly, G. and Weiss, A. (1970b) Arrangement and orientation of cationic surfactants on plane silicate surfaces. 1. Preparation of normal-alkylammonium derivates of mica type laminated silicates. *Kolloid-Zeitschrift und Zeitschrift für Polymere*, **237**, 266−273.

Lagaly, G. and Weiss, A. (1970c) Arrangement and orientation of cationic tensides on silicate surfaces. 3. Paraffin-like structures in alkylammonium layer silicates with an average layer load (vermiculite). *Kolloid-Zeitschrift und Zeitschrift für Polymere*, **238**, 485−493.

Lagaly, G. and Weiss, A. (1971) Anordnung und Orientierung kationischer Tenside auf Silikatoberflächen 4. Anordnung von *n*-Alkylammoniumionen bei niedrig geladenen Schichtsilikaten. *Kolloid-Zeitschrift und Zeitschrift für Polymere*, **243**, 48−55.

Laird, D. and Fleming, P. (2008) Analysis of layer charge, cation and anion exchange capacities, and synthesis of reduced charge clays. Pp. 485−509 in: *Methods of Soil Analysis. Part 5. Mineralogical Methods* (A.L. Ulery and L.R. Drees, editors). Soil Science Society of America, Madison, Wisconsin, USA.

Laird, D.A. and Nater, E.A. (1993) Nature of illitic phase associated with randomly interstratified smectite illite in soils. *Clays and Clay Minerals*, **41**, 280−287.

Laird, D.A., Scott, A.D., and Fenton, T.E. (1989a) Evaluation of the alkylammonium method of determining layer charge. *Clays and Clay Minerals*, **37**, 41−46.

Laird, D.A., Thompson, M.L., and Scott, A.D. (1989b) Technique for transmission electron-microscopy and X-ray-powder diffraction analyses of the same clay mineral specimen. *Clays and Clay Minerals*, **37**, 280–282.

Lee, S.Y. and Kim, S.J. (2002) Expansion of smectite by hexadecyltrimethylammonium. *Clays and Clay Minerals*, **50**, 435–445.

Lee, B.D., Sears, S.K., Graham, R.C., Amrhein, C., and Vali, H. (2003) Secondary mineral genesis from chlorite and serpentine in an ultramafic soil toposequence. *Soil Science Society of America Journal*, **67**, 1309–1317.

Lee, S.Y., Jackson, M.L., and Brown, J.L. (1975) Micaceous occlusions in kaolinite observed by ultramicrotomy and high-resolution electron-microscopy. *Clays and Clay Minerals*, **23**, 125–129.

MacEwan, D.M.C. (1944) Identification of the montmorillonite group of minerals by X-rays. *Nature*, **154**, 577–578.

Maes, A. and Cremers, A. (1977) Charge-density effects in ion-exchange. 1. Heterovalent exchange equilibria. *Journal of the Chemical Society – Faraday Transactions I*, **73**, 1807–1814.

Maes, A., Stul, M.S., and Cremers, A. (1979) Layer charge-cation-exchange capacity relationships in montmorillonite. *Clays and Clay Minerals*, **27**, 387–392.

Malikova, N., Cadene, A., Dubois, E., Marry, V., Durand-Vidal, S., Turq, P., Breu, J., Longeville, S., and Zanotti, J.M. (2007) Water diffusion in a synthetic hectorite clay studied by quasi-elastic neutron scattering. *Journal of Physical Chemistry C*, **111**, 17603–17611.

Malla, P.B. and Douglas, L.A. (1987) Identification of expanding layer silicates: layer charge vs. expansion properties. International Clay Conference, Denver, The Clay Minerals Society, Bloomington, Indiana, pp. 277–283.

Malla, P.B., Robert, M., Douglas, L.A., Tessier, D., and Komarneni, S (1993) Charge heterogeneity and nanostructure of 2:1 layer silicates by high-resolution transmission electron-microscopy. *Clays and Clay Minerals*, **41**, 412–422.

Mermut, A.R. (1994) Problems associated with layer charge characterization of 2:1 phyllosilicates. Pp. 106–122 in: *Layer Charge Characteristics of 2:1 Clay Minerals* (A. Mermut, editor). CMS Workshop Lectures, **6**, The Clay Minerals Society, Boulder, Colorado, USA.

Olis, A.C., Malla, P.B., and Douglas, L.A. (1990) The rapid estimation of layer charges of 2:1 expanding clays from a single alkylammonium ion expansion. *Clay Minerals*, **25**, 39–50.

Rühlicke, G. and Kohler, E.E. (1981) A simplified procedure for determining layer charge by the *n*-alkylammonium method. *Clay Minerals*, **16**, 305–307.

Schultz, L.G. (1969) Lithium and potassium absorption, dehydroxylation temperature, and structural water content of aluminous smectites. *Clays and Clay Minerals*, **17**, 115–149.

Sears, S.K. (2001) The study of crystal structure in the evolution of interstratified 2:1 clay minerals, Reindeer D-27 well, Mackenzie Delta – Beaufort Sea region, Arctic Canada. PhD thesis, McGill University, Montreal, Canada, 271 pp.

Sears, S.K., Hesse, R., and Vali, H. (1998) Significance of n-alkylammonium exchange in the study of 2:1 clay mineral diagenesis, Mackenzie Delta Beaufort Sea region, Arctic Canada. *The Canadian Mineralogist*, **36**, 1485–1506.

Shata, S., Hesse, R., Martin, R.F., and Vali, H. (2003) Expandability of anchizonal illite and chlorite: Significance for crystallinity development in the transition from diagenesis to metamorphism. *American Mineralogist*, **88**, 748–762.

Sinclair, I.K. (1988) Evolution of Mesozoic–Cenozoic sedimentary basins in the Grand Banks area of Newfoundland and comparison with Falvey's (1974) rift model. *Bulletin of Canadian Petroleum Geology*, **36**, 255–273.

Stanjek, H. and Friedrich, R. (1986) The determination of layer charge by curve-fitting of Lorentz- and polarization-corrected X-ray diagrams. *Clay Minerals*, **21**, 183–190.

Stul, M.S. and Mortier, W.J. (1974) The heterogeneity of the charge density in montmorillonites. *Clays and Clay Minerals*, **22**, 391–396.

Vali, H. (1983) Vergleichende elektronenoptische und röntgenographische Untersuchungen zur Kristallstruktur und Morphologie von quellfühigen und nicht quellenden 2:1-Schichtsilikaten. PhD, Technische Universität München, Germany, 94 pp.

Vali, H. and Hesse, R. (1990) Alkylammonium ion treatment of clay minerals in ultrathin sections – A new method for HRTEM examination of expandable layers. *American Mineralogist*, **75**, 1443–1446.

Vali, H. and Hesse, R. (1992) Identification of vermiculite by transmission electron microscopy and X-ray diffraction. *Clay Minerals*, **27**, 185–192.

Vali, H. and Köster, H.M. (1986) Expanding behavior, structural disorder, regular and random irregular interstratification of 2:1 layer silicates studied by high-resolution images of transmisson electron microscopy. *Clay Minerals*, **21**, 827–859.

Vali, H., Hesse, R., and Kohler, E.E. (1991) Combined freeze-etch replicas and HRTEM images as tools to study fundamental particles and the multiphase nature of 2:1 layer silicates. *American Mineralogist*, **76**, 1973–1984.

Vali, H., Martin, R.F., Amarantidis, G., and Morteani, G. (1993) Smectite-group minerals in deep-sea sediments – Monomineralic solid-solutions or multiphase mixtures? *American Mineralogist*, **78**, 1217–1229.

Vali, H., Hesse, R., and Martin, R.F. (1994) A TEM-based definition of 2:1 layer silicates and their interstratified constituents. *American Mineralogist*, **79**, 644–653.

Vogt, K. and Köster, H.M. (1978) Mineralogy, crystallography and geochemistry of some montmorillonites from bentonites. *Clay Minerals*, **13**, 25–43.

(*Received 24 July 2013; revised 27 September 2014; Ms. 792; AE: P.B. Malla*)